8250–8260 *Nucleic Acids Research, 2016, Vol. 44, No. 17* *Published online 20 June 2016*
doi: 10.1093/nar/gkw563

PCNA tool belts and polymerase bridges form during translesion synthesis

Elizabeth M. Boehm, Maria Spies and M. Todd Washington*

Department of Biochemistry, Carver College of Medicine, University of Iowa, Iowa City, IA 52242, USA

Received March 11, 2016; Revised June 9, 2016; Accepted June 10, 2016

ABSTRACT

Large multi-protein complexes play important roles in many biological processes, including DNA replication and repair, transcription, and signal transduction. One of the challenges in studying such complexes is to understand their mechanisms of assembly and disassembly and their architectures. Using single-molecule total internal reflection (TIRF) microscopy, we have examined the assembly and disassembly of the multi-protein complex that carries out translesion synthesis, the error-prone replication of damaged DNA. We show that the ternary complexes containing proliferating cell nuclear antigen (PCNA) and two non-classical DNA polymerases, Rev1 and DNA polymerase η, have two architectures: PCNA tool belts and Rev1 bridges. Moreover, these complexes are dynamic and their architectures can interconvert without dissociation. The formation of PCNA tool belts and Rev1 bridges and the ability of these complexes to change architectures are likely means of facilitating selection of the appropriate non-classical polymerase and polymerase-switching events.

INTRODUCTION

DNA damage, which arises from endogenous and exogenous sources, blocks the progression of replication forks. Translesion synthesis (TLS) is a pathway used to overcome these replication blocks. It involves the use of specialized, non-classical DNA polymerases that are capable of replicating through DNA damage (1–5). During TLS, a large multi-protein complex containing these non-classical DNA polymerases is assembled at stalled replication forks (6,7). Core structural components of this complex are the replication accessory factor proliferating cell nuclear antigen (PCNA) and the non-classical polymerase Rev1. These are both hub proteins that are responsible for recruiting other non-classical polymerases to sites of stalled replication (6–19).

PCNA is an essential replication accessory factor that orchestrates many events at the replication fork (20,21). This ring-shaped protein encircles double-stranded DNA and acts as a sliding clamp during DNA replication (22). It interacts with and regulates the function of many proteins involved in DNA replication and repair. Most of these replication and repair proteins contain a PCNA-interacting protein (PIP) motif. These short, conserved sequence motifs bind in a hydrophobic pocket on the front face of the PCNA ring (20,23–25). Because PCNA is a homo-trimer, it can potentially act as a tool belt and interact with multiple binding partners simultaneously.

Rev1 is a non-classical polymerase that carries out two distinct functions in TLS. First, its catalytic function is responsible for incorporating cytosine opposite minor-groove and exocyclic guanine adducts and abasic sites (26–29). Second, its non-catalytic function is responsible for binding and organizing other non-classical polymerases within the multi-protein TLS complex (14–18,30). Most of these non-classical polymerases contain a PIP-like motif called a Rev1-interacting region (RIR) motif (18,31). These short sequence motifs bind in a hydrophobic pocket on the C-terminal domain of Rev1 (6,7,19).

DNA polymerase η (pol η) is the best understood of the non-classical polymerases. It is responsible for incorporating nucleotides opposite 8-oxoguanines and ultraviolet radiation-induced thymine-thymine dimers (32,33). Loss of pol η function in humans is responsible for the cancer-prone genetic disorder xeroderma pigmentosum variant form (XPV) (34,35). Like Rev1, pol η is believed to be one of the first non-classical polymerases recruited to stalled replication forks and can be considered a 'first responder' (4).

The arrangement of the component proteins (i.e. the architecture) of this multi-protein TLS complex is poorly understood. In the yeast system, the PIP motif of pol η has two roles. It mediates the interaction of pol η and PCNA, and it functions as a RIR motif to mediate the interaction of pol η and Rev1 (8,36). Given the dual role of this PIP motif, it is unlikely that pol η can directly interact with both PCNA and Rev1 at the same time. Thus, there are only two expected architectures of the PCNA–Rev1–pol η ternary complex: a PCNA tool belt or a Rev1 bridge. In a PCNA tool belt, pol η directly binds to PCNA and PCNA directly binds

*To whom correspondence should be addressed. Tel: +1 319 335 7518; Fax: +1 319 335 9570; Email: todd-washington@uiowa.edu

to Rev1, but pol η does not directly bind to Rev1. In a Rev1 bridge, pol η directly binds to Rev1 and Rev1 directly binds to PCNA, but pol η does not directly bind to PCNA.

To determine whether PCNA tool belts or Rev1 bridges form and to determine their mechanism of assembly and disassembly, we used single-molecule total internal reflection fluorescence (TIRF) microscopy. We provide, to our knowledge, the first evidence that eukaryotic proteins form PCNA tool belts and Rev1 bridges. Moreover, we show that these ternary complexes are dynamic, with PCNA tool belts switching to Rev1 bridges and vice versa without dissociation. The formation of tool belts and bridges and the ability of these complexes to change architectures are likely means of facilitating the selection of the appropriate non-classical polymerase and facilitating the polymerase-switching events that occur during TLS.

MATERIALS AND METHODS

Protein expression and purification

The wild-type yeast pol η protein was produced as an N-terminal glutathione-s-transferase (GST) fusion protein in yeast strain BJ5464 harboring plasmid pKW546. This protein contained an Avi tag (GLNDIFEAQKIEWHE) inserted between the PreScission protease cleavage site used to remove the GST tag and the N-terminus of pol η. These yeast cells also harbored plasmid pKW547 from which the *Escherichia coli* BirA biotin ligase was produced. This resulted in site-specific biotinylation of the Avi tag of pol η at the indicated lysine residue when the cells were grown in the presence of 0.1 mM biotin. Otherwise, biotinylated pol η was produced, the GST tag was removed, and the protein was purified as described previously (37). The mutant pol η protein with substitutions in the PIP motif (S621A, F627A, F628A) was produced the same way using plasmid pKW560.

The wild-type yeast Rev1 protein was produced as an N-terminal GST fusion protein in yeast strain BJ5464 harboring plasmid pKW143. Rev1 was produced, the GST tag was removed and the protein was purified as described previously (38). The mutant Rev1 protein with substitutions in the CTD motif (L889A, W893A, T897A, L898A, V910A) was produced the same way using plasmid pKW570. The mutant Rev1 protein with a substitution in the BRCA1 C-terminus (BRCT) domain (G193R) was produced the same way using plasmid pKW665.

Wild-type yeast PCNA was produced as an N-terminal His_6 tag in *E. coli* BL21 DE3 cells harboring plasmid pKW336. This protein was produced and purified as described previously (39). The mutant PCNA protein with substitutions in its PIP binding pocket (I128A, P234A, P252A) was produced the same way using plasmid pKW559.

Fluorescent labeling of PCNA and Rev1

Purified yeast PCNA and Rev1 were dialyzed in buffer containing 50 mM potassium phosphate, pH 7.05, 100 mM sodium chloride and 1 mM dithiolthreitol. In the case of PCNA, protein solutions (5–15 μM in 200 μl) were then incubated with 1 mg of Cy3 NHS ester (GE Healthcare) solubilized in 10 μl DMSO in darkness for 16 h at 4°C for labeling the protein N-terminus. In the case of Rev1, the protein was labeled with Cy5 NHS ester (GE Healthcare) using the same procedure. In both cases, free dye was removed with Micro Bio-Spin™ six columns (BioRad). Labeling efficiency was determined by comparing the absorbance at 280 nm for protein, 530 nm for Cy3 and 649 nm for Cy5. In both Cys-labeled PCNA and Cy5-labeled Rev1, labeling efficiencies were ∼80%. Labeled PCNA was directly used without freezing, and labeled Rev1 was flash-frozen and stored until use at −80°C.

Single molecule imaging

A prism-type total internal fluorescence (TIRF) microscope was used to obtain single molecule data (40–43). The TIRF microscope was assembled on an Olympus IX-71 frame (Olympus America, Inc.). Diode-pumped solid-state (DPSS) lasers with excitation wavelengths of 532 and 633 nm (Coherent) were aligned using a polarizing cube beam splitter (Melles Griot) and passed through a Pellin-Broca prism (Eksma Optics) to generate an evanescent field for the simultaneous excitation of Cy3 and Cy5. A water immersion 60× objective lens (Olympus) was used to observe fluorescence signals. To remove scattered excitation light in the emission optical pathway, a Cy3/Cy5 dual band-pass filter (Semrock) was used. An EMCCD camera (Andor) was used to record images at ten frames per second and an amplification gain of 290 without binning. Images were chromatically separated into Cy3 and Cy5 images using a 630 nm dichroic mirror inside the dual view system (Photometrics). The power of the green laser at the microscope slide was 45 mW, and the power of the red laser at the slide was 90 mW for all single molecule experiments reported in this study unless otherwise indicated.

Pol η (1 nM) was immobilized on the surface of a microscope slide chamber that was coated with sparsely biotinylated polyethylene glycol and 100 pM neutravidin. After 3 min, excess pol η was removed from the imaging chamber with reaction buffer containing 50 mM Tris chloride (pH 7.5), 150 mM sodium chloride, 0.1 mg/ml bovine serum albumin, 0.8% glucose and 1 mM dithiolthreitol. Cy3-labeled PCNA (1 nM) and Cy5-labeled Rev1 (1 nM) were injected into the image chamber and 300 s videos with 100 ms frames were recorded. We used an oxygen scavenging system with 12 mM Trolox (6-hydroxy-2,5,7,8-tetramethylchromane-2-carboxylic acid) prepared in MilliQ water with 12 mM NaOH and incubated under fluorescent light with continuous rotation for 3–4 days at room temperature as previously described (41,42,44).

Controls experiments were carried out in the absence of immobilized pol η to ensure that all binding events were pol η-dependent. Additional control experiments were also carried out in which the laser power was reduced to half in order to ensure that the losses of fluorescence signals were due to protein dissociation and not bleaching of the fluorophore. The k_{off} values measured for the PCNA–pol η binary complexes and the Rev1–pol η binary complexes were independent of laser power.

Analysis of single-molecule data

We extracted single-molecule fluorescence trajectories from recorded videos as previously described (41,42). Trajectories were selected for further analysis if they demonstrated stable average signal intensities over time (45). QuB was used to separately normalize the Cy3 and Cy5 trajectories and to identify binding events (46). To distinguish genuine binding events from labeled protein diffusing near the slide surface, we only considered increases in fluorescence intensity that persisted for at least two frames (each frame was 0.1 s). The Cy3 and Cy5 QuB output files were combined and analyzed using the Kinetic Event Resolving Algorithm (KERA), software developed in our laboratory specifically for this study. Briefly, KERA aligns each of the idealized Cy3 trajectories with their corresponding Cy5 trajectories. The binding events are then sorted into categories depending on the order of Cy3-association, Cy5-association, Cy3-dissociation and Cy5-dissociation steps that occur within the event. The times of all binding events are extracted in order to analyze residence times. Any events truncated by either the beginnings or the endings of the trajectory are automatically removed from analysis.

RESULTS

Pol η forms binary and ternary complexes with PCNA and Rev1

To understand the mechanisms of assembly and disassembly and the architectures of protein complexes that form among pol η, Rev1 and PCNA, we used single-molecule TIRF microscopy. Yeast pol η was immobilized on the surface of a microscope slide, and Cy3-labeled PCNA (1 nM) and Cy5-labeled Rev1 (1 nM) were added to the slide chamber (Figure 1A). We obtained 1073 fluorescence trajectories—i.e. plots of fluorescence intensities from locations of individual, immobilized pol η molecules as a function of time. A representative fluorescence trajectory is shown in Figure 1B. When the fluorescence intensities in both the Cy3 and Cy5 channels are at the baseline, the immobilized pol η molecule is bound to neither PCNA nor Rev1. Increases in fluorescence intensity above the baseline in the Cy3 channel indicate the association of PCNA with an immobilized pol η, and decreases in intensity to the baseline in the Cy3 channel indicate dissociation of PCNA from the immobilized pol η. Increases and decreases in intensity in the Cy5 channel indicate the association and dissociation of Rev1.

Prior to any pol η-binding event, the fluorescence intensities in both the Cy3 and Cy5 channels are at the baseline. A binding event begins when the intensity in either the Cy3 or Cy5 channel increases above the baseline (i.e. when either PCNA or Rev1 associates with the pol η molecule). Multiple association and dissociation steps are possible during the course of the binding event. The event ends when the intensities in both the Cy3 and Cy5 channels return to the baseline. The trajectory shown in Figure 1B, for example, has six pol η-binding events. The second, third, fifth and sixth events only involve Rev1 binding to the immobilized pol η molecule. The first and fourth events, by contrast, involve both Rev1 and PCNA binding to the pol η molecule.

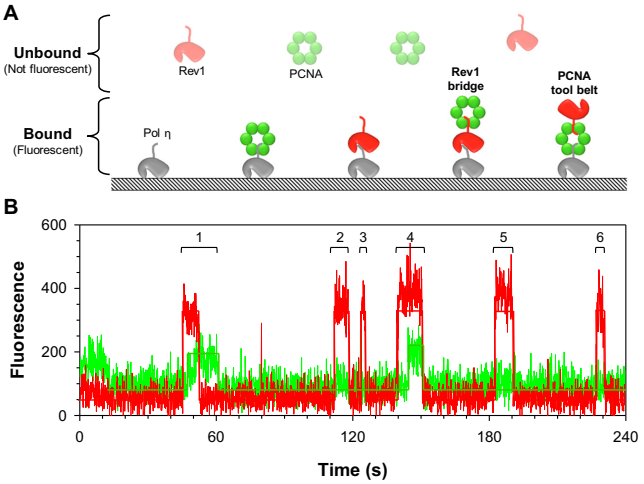

Figure 1. Experimental setup and representative fluorescence trajectory. (**A**) The diagram illustrates the TIRF microscopy experimental setup. Pol η is immobilized on the surface of the microscope slide and Cy3-labeled PCNA and Cy5-labeled Rev1 are added to the slide chamber. Increases and decreases in intensity in the Cy3 channel indicate the association and dissociation of PCNA either directly or indirectly with the immobilized pol η. Increases and decreases in intensity in the Cy5 channel indicate the association and dissociation of Rev1. Diagrams of PCNA tool belt ternary complexes and Rev1 bridge ternary complexes are shown. (**B**) A representative fluorescence trajectory is shown in which the fluorescence intensities in the Cy3 and Cy5 channels from the location of a single, immobilized pol η molecule are graphed as a function of time. Six binding events are indicated. The second, third, fifth and sixth binding events are simple and correspond to Rev1–pol η binary complexes. The first and fourth are complicated and consist of one PCNA–Rev1–pol η ternary complex each. The event at the beginning of the trajectory (0–20 s) was excluded from analysis because the formation of this complex was not observed.

We obtained a total of 8894 pol η-binding events. Because we used very low concentrations of PCNA and Rev1, most of these were simple binding events consisting of a single association step followed by a single dissociation step. For example, 3734 events (42.0%) consisted of a PCNA-association step followed by a PCNA-dissociation step. These events correspond to single pol η–PCNA binary complexes. Similarly, 4400 events (49.5%) consisted of a Rev1-association step followed by a Rev1-dissociation step. These correspond to single pol η–Rev1 binary complexes. The remaining 760 (8.5%) binding events were complicated and consisted of multiple association and dissociation steps. These complicated events all contained at least one pol η–PCNA–Rev1 ternary complex.

The number of simple events per trajectory ranged from one to twenty-six with an average of 7.6 simple events per trajectory (Figure 2A). The total number of trajectories with simple events was 1073 (100%). The number of complicated events per trajectory ranged from zero to seven with an average of 0.7 complicated events per trajectory (Figure 2B). The total number of trajectories with complicated events was 493 (45.9%). This shows that despite the relatively low proportion of complicated events (8.5% of total events), nearly half of the individual pol η molecules examined formed at least one pol η–PCNA–Rev1 ternary complexes during the 5-min observation time.

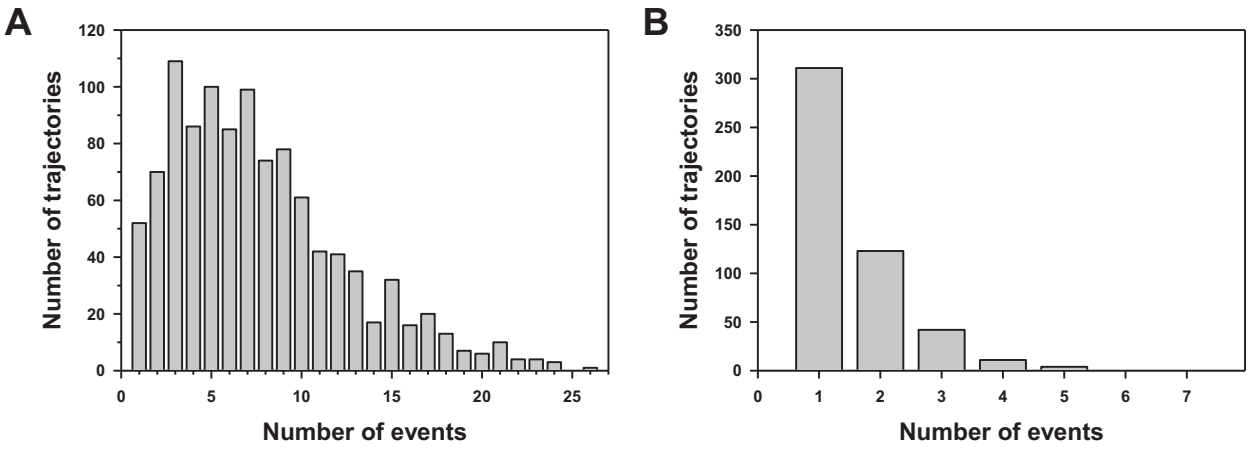

Figure 2. Distribution of the simple and complicated binding events. (**A**) The histogram shows the number of fluorescence trajectories with a given number of simple binding events. The total number of trajectories with simple events was 1073, and the number of simple events per trajectory ranged from 1 to 26 with an average of 7.6 simple events per trajectory. (**B**) The histogram shows the number of trajectories with a given number of complicated events. The total number of trajectories with complicated events was 493, and the number of complicated events per trajectory ranged from one to seven with an average of 0.7 complicated events per trajectory.

Formation of both binary and ternary complexes depend on the PIP motif of pol η

We previously showed that the PIP motif of yeast pol η mediates its interaction both with PCNA and with Rev1 (36). To show that the formation of ternary complexes between pol η, PCNA and Rev1 was dependent on the pol η PIP motif, we carried out identical single-molecule TIRF experiments as described above, except using an immobilized pol η mutant protein with substitutions in the PIP motif (S621A, F627A, F628A). This mutant protein greatly reduces the affinity of pol η for both PCNA and Rev1 (8,36). We obtained 329 total pol η binding events with the mutant pol η protein compared to the 8894 total pol η-binding events observed with the wild-type pol η protein under the same conditions. Of these, 149 were simple events corresponding to PCNA–pol η binary complexes, 141 were simple events corresponding to single Rev1–pol η binary complexes and 39 were complicated events containing a single pol η–PCNA–Rev1 ternary complex. These results show that the PIP motif of pol η plays an important role in mediating the interactions between pol η and Rev1 and between pol η and PCNA in the binary as well as the ternary complexes.

The PIP motif of pol η can bind to a hydrophobic pocket on the front surface of the PCNA ring or to a hydrophobic pocket on the C-terminal domain of Rev1 (36). Given the structural bases of these interactions, it is highly unlikely that the PIP motif of pol η can bind to both PCNA and Rev1 simultaneously. Thus, pol η cannot directly interact with both PCNA and Rev1 at the same time. This means that there are only two expected architectures of the ternary complexes formed by these proteins: Rev1 bridges and PCNA tool belts (see Figure 1A). In a Rev1 bridge, pol η directly binds to Rev1 and not to PCNA. Instead, PCNA binds to Rev1 at a different site than pol η does and Rev1 acts as a bridge linking pol η and PCNA. In a PCNA tool belt, pol η directly binds to PCNA, and not to Rev1. Rev1 binds to PCNA at a different site than pol η does, and PCNA acts as a tool belt linking pol η and Rev1.

The ternary complexes include both PCNA tool belts and Rev1 bridges

The 8894 binding events were sorted into 44 classes based on the number, type and order of their component association and dissociation steps. Two of these classes corresponded to the two aforementioned types of simple events (8134 events). Forty-two of these classes corresponded to complicated events (760 events). Figure 3 shows representative trajectories for the six most common classes of binding events. The full catalog of binding events is shown as idealized trajectories in Supplementary Figure S1. As described above, the class A and class B events correspond to PCNA–pol η binary complexes and Rev1–pol η binary complexes, respectively.

Class C events are the most common type of complicated event (36.8%), and these each contain a single PCNA–Rev1–pol η ternary complex (Figure 3C). Class C events begin when a PCNA molecule associates with an immobilized pol η molecule to form a PCNA–pol η binary complex. Rev1 then associates with this binary complex to form a PCNA–Rev1–pol η ternary complex. The order of assembly of this complex is most consistent with a ternary complex possessing a PCNA-tool-belt architecture. This is because the pol η PIP motif is occupied in the PCNA–pol η binary complex and would not be available for binding Rev1. The most direct way that Rev1 can bind to this binary complex is to interact directly with PCNA, not with pol η. Class C events end when a Rev1 molecule dissociates from the PCNA–Rev1–pol η ternary complex leaving behind a PCNA–pol η binary complex. PCNA then dissociates from this binary complex leaving behind a free pol η. The order of disassembly of this ternary complex is also most consistent with a PCNA-tool-belt architecture.

Class D events are the second most common type of complicated event (16.3%), and each contains a single ternary complex (Figure 3D). These events begin when a Rev1 molecule associates with a pol η molecule to form a Rev1–pol η binary complex. PCNA then associates with this bi-

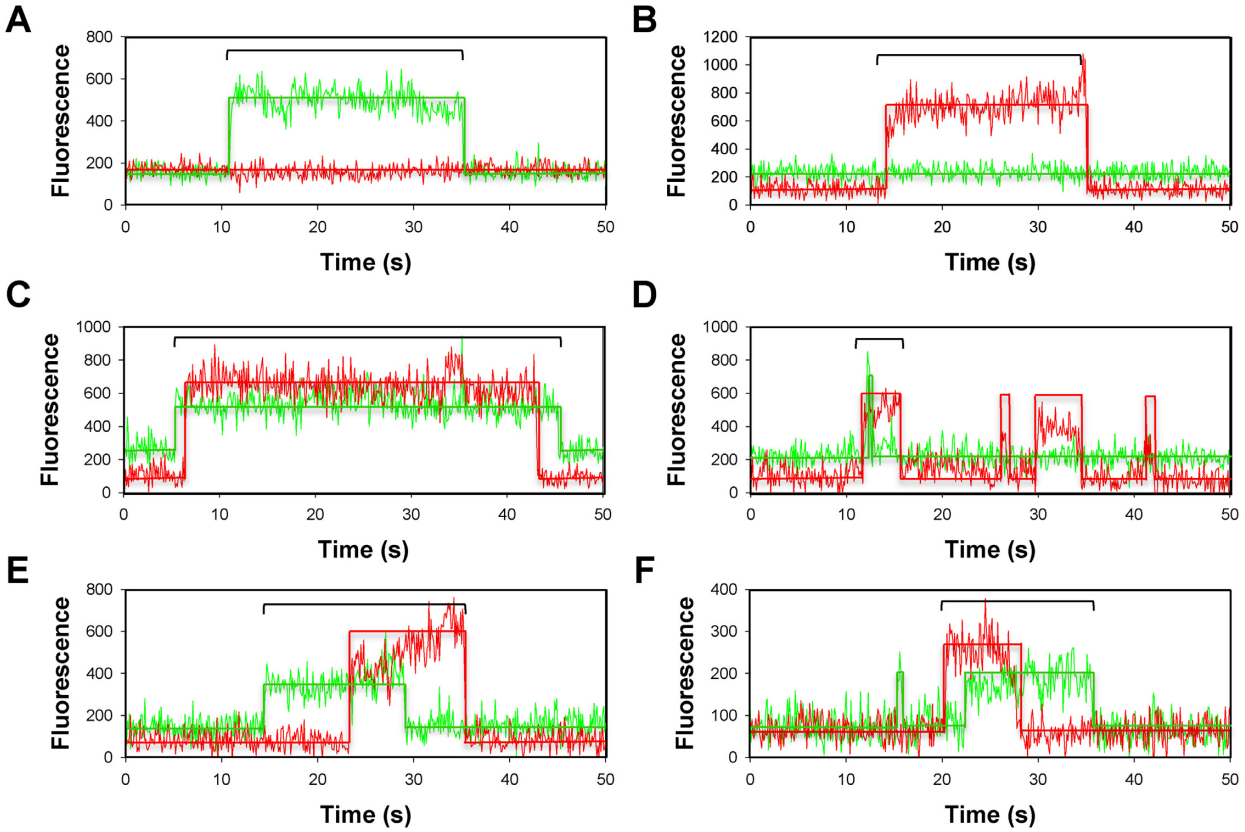

Figure 3. The six most common binding events. (**A**) A representative simple binding event corresponding to a single PCNA–pol η binary complex. We observed 3734 events of this type. (**B**) A representative simple binding event corresponding to a single Rev1–pol η binary complex. We observed 4400 events of this type. (**C**) A representative complicated binding event corresponding to a single PCNA–Rev1–pol η ternary complex with a PCNA tool belt architecture. We observed 218 events of this type. (**D**) A representative complicated event corresponding to a single PCNA–Rev1–pol η ternary complex with a Rev1 bridge architecture. We observed 124 events of this type. (**E**) A representative complicated event corresponding to a single PCNA–Rev1–pol η ternary complex with an architecture switching from a PCNA tool belt to a Rev1 bridge. We observed 57 events of this type. (**F**) A representative complicated event corresponding to a single PCNA–Rev1–pol η ternary complex with an architecture switching from a Rev1 bridge to a PCNA tool belt. We observed 56 events of this type.

nary complex to form a ternary complex. The order of assembly of this complex is most consistent with a ternary complex possessing a Rev1-bridge architecture. This is because the pol η PIP motif is occupied in the Rev1–pol η binary complex and would not be available for binding PCNA. The most direct way that PCNA can bind to this binary complex is to interact directly with Rev1, not with pol η. These events end when a PCNA molecule dissociates from the PCNA–Rev1–pol η ternary complex leaving behind a Rev1–pol η binary complex. Rev1 then dissociates leaving behind free pol η. The order of disassembly of this ternary complex is also most consistent with a Rev1-bridge architecture.

Overall, the 760 total complicated pol η-binding events grouped into 42 classes contain a total of 971 ternary complexes (Supplementary Figure S1). The number of ternary complexes per complicated event ranged from 1 to 10 with an average of 1.3 ternary complexes per complicated binding event. Examination of the order of assembly and disassembly of each of these ternary complexes shows that 375 ternary complexes (38.6%) were PCNA tool belts and 222 (22.9%) were Rev1 bridges (Figure 4).

PCNA tool belts and Rev1 bridges are capable of interconverting

Class E events are less common (7.5%); these each contain a single PCNA–Rev1–pol η ternary complex (Figure 3E). These events begin when a PCNA molecule associates with an immobilized pol η molecule to form a PCNA–pol η binary complex. Rev1 then associates with this binary complex to form a PCNA–Rev1–pol η ternary complex. The order of assembly of this complex indicates a PCNA tool belt. These events end, however, when a PCNA molecule dissociates from the PCNA–Rev1–pol η ternary complex leaving behind a Rev1–pol η binary complex. Rev1 then dissociates from this binary complex leaving behind a free pol η. The order of disassembly of this ternary complex indicates a Rev1 bridge. We believe that these complexes assemble as a PCNA tool belt and then switch to a Rev1 bridge before dissociating. This shows that the ternary complexes are dynamic and can switch architectures without dissociating.

Occurring at nearly the same frequency are Class F events (7.4%); these also contain a single PCNA–Rev1–pol η ternary complex (Figure 3F). These events begin when a Rev1 molecule associates with an immobilized pol

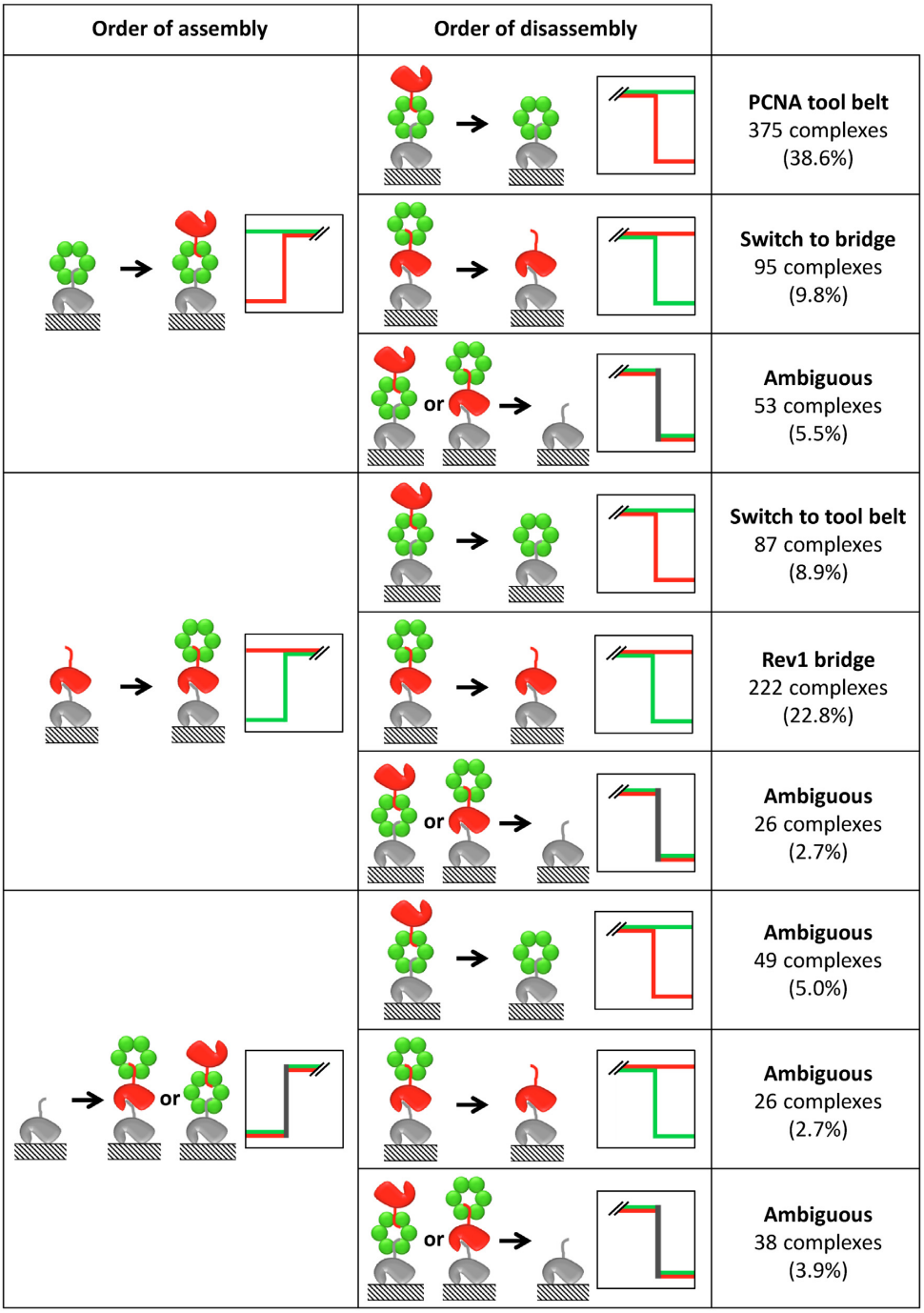

Figure 4. The types of ternary complexes. Diagrams and partial idealized trajectories are shown for the three possible orders of assembly for a ternary complex and for the three possible orders of disassembly of the ternary complexes. For each pathway of ternary complex assembly and disassembly, the number of complexes and the implied architecture (PCNA tool belt, Rev1 bridge, switch from tool belt to bridge, switch from bridge to tool belt and ambiguous) is given.

η molecule to form a Rev1–pol η binary complex. PCNA then associates to form a PCNA–Rev1–pol η ternary complex. The order of assembly of this complex indicates a Rev1 bridge. These events end, however, when a Rev1 molecule dissociates first followed by PCNA dissociation. The order of disassembly of this ternary complex indicates a PCNA tool belt. We believe that these complexes assemble as a Rev1 bridge and then switch to a PCNA tool belt. Again, this suggests that the ternary complexes are dynamic and can re-arrange their architectures without dissociating.

Examination of the order of assembly and disassembly of all of the ternary complexes in all complicated binding events showed that 95 complexes (9.8%) involved a switch from a PCNA tool belt to a Rev1 bridge. Moreover, 87 complexes (8.9%) involved a switch from a Rev1 bridge to a PCNA tool belt (Supplementary Figure S1 and Figure 4).

The remaining 192 of the 971 ternary complexes (19.8%) either assembled by a pre-formed PCNA–Rev1 complex associated with an immobilized pol η molecule or disassembled by a PCNA–Rev1 complex dissociating from pol η. In these cases, either the order of assembly or disassembly was uninformative. We therefore consider the architectures of these complexes to be ambiguous (Figure 4).

The formation of ternary complexes depends on the BRCT domain of Rev1 and on the PIP binding pocket of PCNA

To directly demonstrate that these ternary complexes were PCNA tool belts and Rev1 bridges, we carried out identical single-molecule TIRF experiments as described above, except using a mutant Cy5-labeled Rev1 protein with a substitution in the BRCT domain (G193R), which greatly reduces affinity of Rev1 for PCNA (12). This substitution disrupts direct interactions between Rev1 and PCNA without affecting the interactions between Rev1 and pol η. Because this interaction is necessary for forming both PCNA tool belts and Rev1 bridges, we expect that this substitution should greatly reduce the number of ternary complexes. Whereas we observed 971 ternary complexes with wild-type proteins, we observed only 74 ternary complexes with the Rev1 BRCT domain mutant protein (Table 1).

We further carried out single-molecule TIRF experiments as described above, except using a mutant Cy3-labeled PCNA protein with a substitution in the PIP motif-binding pocket (I128A, P234A, P252A). Both the PIP motif of pol η and the BRCT domain of Rev1 bind to PCNA in this region (47). These substitutions disrupt direct interactions between PCNA and pol η and between PCNA and Rev1. Because these interactions are necessary for forming both PCNA tool belts and Rev1 bridges, we expect that these substitutions should greatly reduce the number of ternary complexes. We observed only 161 ternary complexes with the PCNA mutant protein compared to 971 with wild-type proteins (Table 1). Taken together, these results strongly support the notion that the ternary complexes are in fact PCNA tool belts and Rev1 bridges.

Substitutions in the CTD of Rev1 affect Rev1 bridges, but not PCNA tool belts

To further verify that these ternary complexes were Rev1 bridges and PCNA tool belts, we carried out additional single-molecule TIRF experiments as described above, except using a mutant Cy5-labeled Rev1 protein with substitutions in the hydrophobic pocket within the C-terminal domain (L889A, W893A, T897A, L898A, V910A), which greatly reduces affinity of Rev1 for binding the pol η PIP motif (36). These substitutions disrupt direct interactions between Rev1 and pol η without affecting the interactions between Rev1 and PCNA. Because this interaction is necessary for forming Rev1 bridges, but not PCNA tool belts, we expect that these substitutions should greatly reduce the number of Rev1 bridges observed, but not the number of PCNA tool belts. Whereas we observed 222 Rev1 bridges with wild-type proteins, we observed only 18 Rev1 bridges with the Rev1 mutant protein (Table 1). Moreover, whereas we observed 375 PCNA tool belts with wild-type proteins, we observed 459 PCNA tool belts with the Rev1 mutant protein. These results provide compelling support for these ternary complexes being Rev1 bridges and PCNA tool belts.

Kinetics of ternary complex assembly and disassembly

From the data presented here, we can directly determine the rate constant of dissociation (k_{off}) of PCNA from the PCNA–pol η binary complex and the k_{off} of Rev1 from the Rev1–pol η binary complex. Figure 5A shows the number of PCNA–pol η binary complexes with a given residence time. From the best fit of this data to an exponential equation, we obtained a k_{off} for PCNA from a PCNA–pol η binary complex that equals 0.53 s^{-1}. Similarly, Figure 5B shows the number of Rev1–pol η binary complexes with a given residence time. From the best fit of this data to an exponential equation, we obtained a k_{off} for Rev1 dissociating from a binary complex that equals 0.73 s^{-1}.

We can also directly determine the k_{off} of PCNA from the PCNA–Rev1–pol η ternary complex (i.e. the Rev1 bridge) and the k_{off} of Rev1 from the PCNA–Rev1–pol η ternary complex (i.e. the PCNA tool belt). Figure 5C shows the number of Rev1 bridge ternary complexes with a given residence time. The best fit of the data yields a k_{off} for PCNA from a Rev1 bridge that equals 0.55 s^{-1}. Likewise, Figure 5D shows the number of PCNA tool belt ternary complexes with a given residence time. The best fit of the data yields a k_{off} that equals 1.2 s^{-1}.

If one assumes that these association and dissociation steps can be described by a simple kinetic partitioning, we can calculate apparent rate constant of association (k_{on}) values from the observed frequencies of the various types of complexes (Supplementary Figure S2). For example, consider each PCNA–pol η binary complex, whether it is in a simple binding event or a complicated binding event. This binary complex can terminate by only one of two ways. Either it can end by a PCNA-dissociation step, which would conclude the entire binding event, or it can end by a Rev1-association step to form a PCNA tool belt ternary complex. Our data shows that the formation of a PCNA–pol η binary complex is followed by PCNA dissociation 89% of the time and is followed by Rev1 association 11% of the time. Given that the k_{off} for PCNA dissociation from the binary complex is 0.53 s^{-1}, we calculate that the observed rate (v_{on}) of association of Rev1 equals 0.066. This corresponds to an apparent k_{on} for Rev1 binding the PCNA–pol η binary complex to form a PCNA tool belt ternary complex that equals 6.6×10^7 $M^{-1}s^{-1}$. Given that the k_{off} for Rev1 dissociating from the PCNA tool belt (1.2 s^{-1}), the apparent dissociation constant (K_d) for Rev1 in a PCNA tool belt equals 18 nM.

Similar calculations yielded a v_{on} of association of PCNA with a Rev1–pol η binary complex to form a Rev1 bridge that equals 0.055 s^{-1}. This corresponds to an apparent k_{on} for PCNA binding to form a Rev1 bridge that equals 5.5×10^7 $M^{-1}s^{-1}$. Given that the k_{off} for PCNA dissociating from a Rev1 bridge (0.55 s^{-1}), the apparent K_d for PCNA in a Rev1 bridge equals 10 nM.

Next, we compared the duration of the PCNA tool belts and Rev1 bridges to the duration of the ternary complexes in which the architecture switches from PCNA tool belts to

Table 1. Distributions of ternary complexes with wild-type and mutant proteins

	Wild-type proteins	Pol η PIP mutant	Rev1 BRCT mutant	Rev1 CTD mutant	PCNA mutant
PCNA tool belts	375	12	23	459	55
Rev1 bridges	222	7	3	18	58
Switches to tool belt	87	3	18	7	20
Switches to bridge	95	5	11	2	17
Ambiguous	192	12	19	30	11
Total	971	39	74	516	161

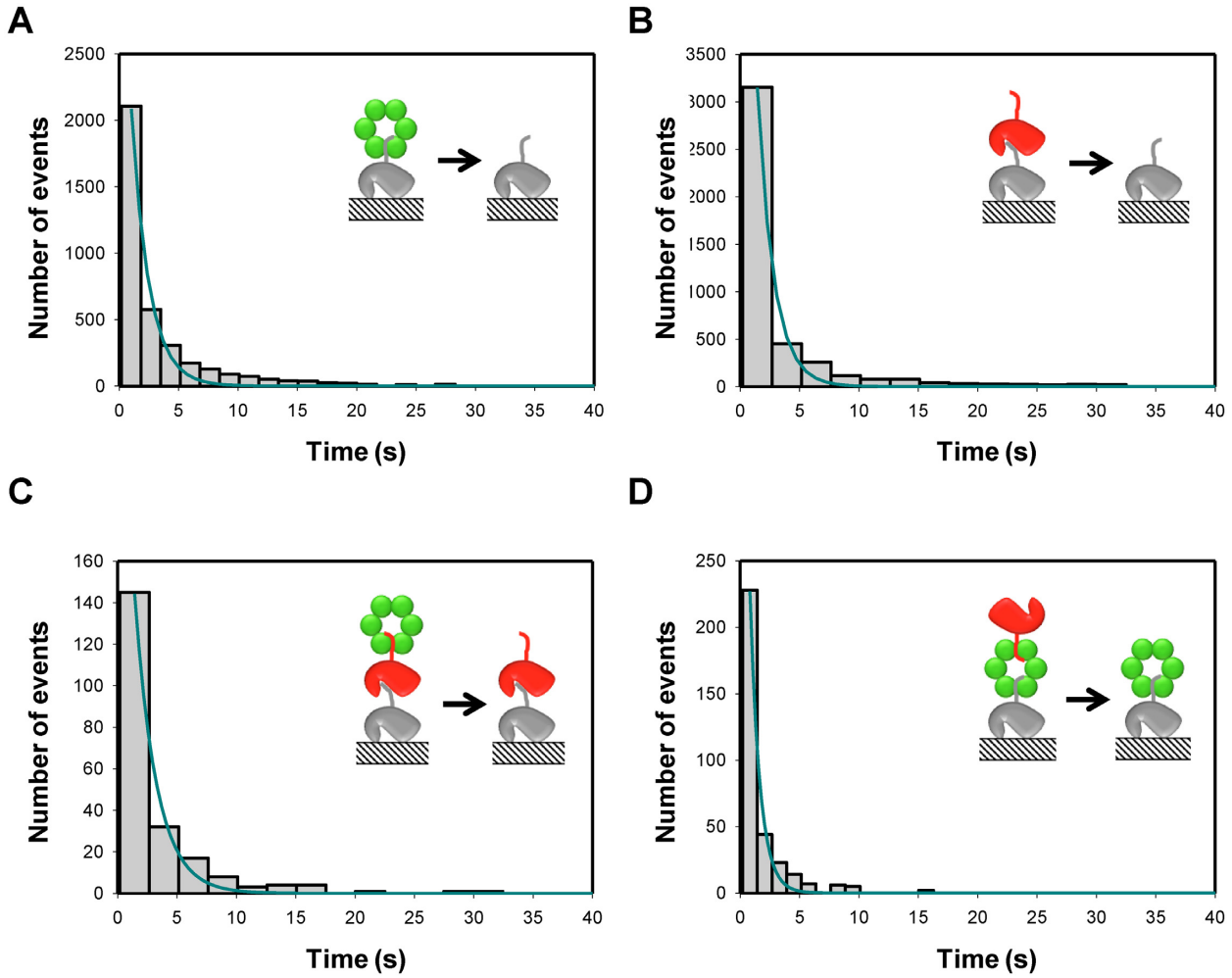

Figure 5. Kinetics of binary and ternary complex dissociation. (**A**) The histogram shows the number of PCNA–pol η binary complexes with a given residence time. The data fit best with a single exponential equation with a k_{off} equal to 0.53 ± 0.01 s^{-1} (solid line). (**B**) The histogram shows the number of Rev1–pol η binary complexes with a given residence time. The data fit best with a single exponential equation with a k_{off} equal to 0.73 ± 0.02 s^{-1} (solid line). (**C**) The histogram shows the number of Rev1 bridge ternary complexes with a given residence time. The data fit best with a single exponential equation with a k_{off} equal to 0.55 ± 0.02 s^{-1} (solid line). (**D**) The histogram shows the number of PCNA tool belt ternary complexes with a given residence time. The data fit best with a single exponential equation with a k_{off} equal to 1.2 ± 0.1 s^{-1} (solid line).

Rev1 bridges or from bridges to tool belts (Figure 6). For example, the median residence time for PCNA tool belts is 0.6 s, while the median residence time for switches from tool belts to bridges is 2.3 s. By comparing the residence times of individual tool belts to the residence times of individual switches from tool belts to bridges, we find that the increased length of the switches is statistically significant in this case ($P < 0.0001$). This suggests that the switching step from tool belt to bridge is partly rate limiting. By contrast, the median residence time for Rev1 bridges is 1.4 s, while the median residence time for switches from bridges to tool belts is 1.1 s. By comparing the residence times of these individual complexes, however, we find that the difference in length is not statistically significant in this case ($P = 0.1837$). Thus the switching step from bridge to tool belt is not rate limiting.

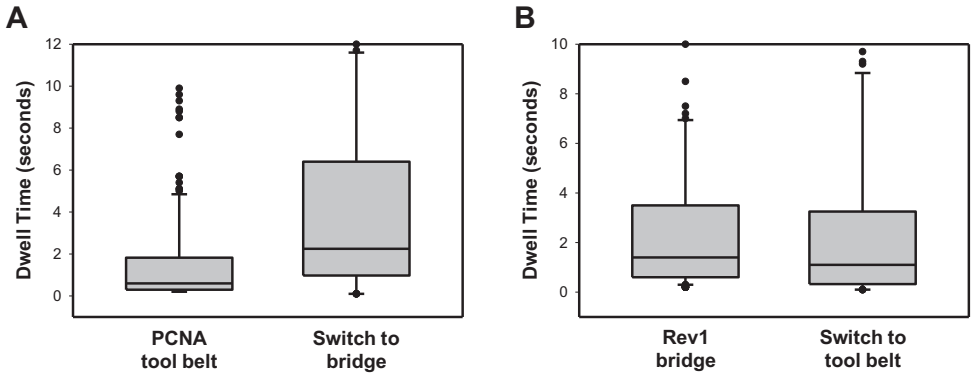

Figure 6. Comparison of the residence time of the ternary complexes. (**A**) Box and whisker plots show the different residence times for PCNA tool belt ternary complexes (left) and ternary complexes that switch from tool belt to bridge (right). The median values for the residence times of these complexes are 0.6 and 2.3 s, respectively. A Mann–Whitney (non-parametric) test indicated that the differences between these residence times are statistically significant ($P < 0.0001$). (**B**) Box and whisker plots show the different residence times for Rev1 bridge ternary complexes (left) and ternary complexes that switch from bridge to tool belt (right). The median values for the residence times of these complexes are 1.4 and 1.1 s, respectively. A Mann–Whitney (non-parametric) test indicated that the differences between these residence times are not statistically significant ($P = 0.1837$).

DISCUSSION

PCNA and Rev1 are the core structural components of the large, multi-protein complex that assembles at stalled replication forks and carries out TLS. Here we used single-molecule TIRF microscopy to examine the formation of binary and ternary complexes between these structural proteins and the prototypical non-classical polymerase, pol η. We provide, for the first time to our knowledge, evidence that these proteins form PCNA tool belt and polymerase bridge ternary complexes. Moreover, we show that these ternary complexes are dynamic and that PCNA tool belts can switch into Rev1 bridges and *vice versa* without the dissociation of any of the components. Such interconversions likely involve, in addition to the primary PIP-mediated contacts, transient secondary contacts either between pol η and PCNA or between pol η and Rev1. The dynamic nature of this complex may play an important role in facilitating the choice of the appropriate polymerase for carrying out TLS and for facilitating the polymerase-switching events that must occur during TLS.

We observed that the majority of the pol η-binding events corresponded to PCNA-pol η binary complexes or Rev-pol η binary complexes. Only a small fraction (8.5%) of the binding events contained one or more ternary complexes. This was the case because we intentionally used low concentrations of PCNA and Rev1 in the microscope slide chamber. This was done for two reasons. First, using higher concentrations of Cy3-labeled PCNA and Cy5-labeled Rev1 would have increased the background and reduced the sensitivity of the single-molecule measurements. Second, using more PCNA and Rev1 would have increased the proportion of PCNA–Rev1 binary complexes that formed in the slide chamber. This would have led to more binding events where PCNA and Rev1 bind to the immobilized pol η simultaneously. In such a case, we would have obtained a far greater percentage of ternary complexes with ambiguous architectures, and this would have limited the amount of useful information we could have extracted regarding the architecture and dynamics of the ternary complexes, the order of assembly and disassembly of these complexes, and the frequencies of each type of complex.

The concentrations of PCNA and Rev1 used in this study (1 nM each) are far below their estimated concentrations *in vivo*. From the estimated number of copies of each protein, the concentration of PCNA, Rev1, and pol η in a yeast nucleus is 5 μM, 250 nM and 900 nM, respectively (48,49). These concentrations are far above the K_d values for these interactions. From the k_{on} and k_{off} values reported here and in our previous study (36), the K_d values for PCNA binding pol η and for PCNA binding the Rev1–pol η binary complex (i.e. forming a Rev1 bridge) are 4.6 and 10 nM, respectively. Similarly, the K_d values for Rev1 binding pol η and for Rev1 binding the PCNA–pol η binary complex (i.e. forming a PCNA tool belt) are 4.5 and 18 nM, respectively. Although these values have been measured at low protein concentrations without the molecular crowding that occurs in the nucleus, we still expect these K_d values to be reasonable approximations of the binding affinities in the cellular context. Given this, the interactions of these three proteins with one another would be under stoichiometric conditions *in vivo*. Provided that these proteins are not all bound up in higher affinity complexes, these proteins would form ternary complexes—both tool belt and Rev1 bridges—at stalled replication forks with very few, if any binary complexes.

While we have focused here on the three core components of the multi-protein TLS complex, other macromolecules are part of this complex *in vivo*. These include other non-classical polymerases such as B-family DNA polymerase ζ (pol ζ), DNA polymerase ι (pol ι) and DNA polymerase κ (pol κ). These also include the Rad6–Rad18 complex, which interacts with pol η (50) and catalyzes the mono-ubiquitylation of PCNA (51,52), and the Mms2–Ubc13–Rad5 complex, which interacts with Rev1 (53) and catalyzes the K63-linked poly-ubiquitylation of PCNA (51,52). The functional significance of the mono-ubiquitylation and poly-ubiquitylation of PCNA in TLS remains unclear. Nevertheless, the single-molecule TIRF microscopy approach with differentially labeled proteins that we used here could

be extended to examine the architecture and mechanism of assembly and disassembly of complexes with these additional components. The data presented here would serve as a critical reference point for these future studies.

The multi-protein TLS complex also includes the DNA substrate, which we left out of these experiments because our focus was the protein-protein interactions within this complex. The inclusion of DNA would also have drastically limited the amount of mechanistic information that we could extract from the data due to the abilities of all three proteins to directly bind DNA. The single-molecule approach would have to be altered substantially in order to extend these studies to examine the architecture and mechanism of assembly and disassembly of complexes in the presence of DNA. Thus, some questions remain regarding how the findings reported here would apply in a real situation when DNA is present. Nevertheless, we believe that the overall architectures and the dynamics of the ternary complexes that we observed here are similar to what would occur in cells at stalled replication forks.

The PCNA tool belt and Rev1 bridge architectures are of significant biological importance. They provide a means of increasing the local concentrations of the non-classical polymerases at stalled replication forks. Given that there are a variety of non-classical polymerases—each with one or a set of closely related cognate lesions—the primer terminus adjacent to the template DNA lesion would have to sample multiple non-classical polymerases to find the appropriate one. Moreover, there is a distinction between non-classical polymerases that carry out the direct incorporation of nucleotides opposite the template lesion (the 'inserters') and those that carry out subsequent nucleotide incorporations (the 'extenders'). This necessitates a polymerase-switching event between the polymerase that functions as the inserter and the polymerase that functions as the extender in order to complete TLS.

The relatively short lifetimes of the binary and ternary complexes that we observed here (∼1–2 s) are likely important for polymerase sampling and polymerase switching. During DNA replication, PCNA remains associated with regions of damaged DNA for several minutes (54). Thus, we envision that in cells, PCNA is stably bound to the damaged DNA while various non-classical polymerases rapidly associate with and dissociate from it thereby constantly forming PCNA tool belts and Rev1 bridges. The formation of PCNA tool belts and Rev1 bridges, and the ability of these complexes to switch between tool belts and bridges and vice versa, is likely the means of facilitating both the selection of the appropriate non-classical polymerase and the polymerase-switching events.

SUPPLEMENTARY DATA

Supplementary Data are available at NAR Online.

ACKNOWLEDGEMENT

We thank Christine Kondratick, Kyle Powers, Melissa Gildenberg, Brittany Ripley, Bret Freudenthal and Lynne Dieckman for valuable discussion.

FUNDING

National Institute of Health [R01 GM108027, R01 GM081433, T32 GM067795]. Funding for open access charge: National Institute of Health [R01 GM108027, R01 GM081433].
Conflict of interest statement. None declared.

REFERENCES

1. Ohmori,H., Friedberg,E. C., Fuchs,R. P., Goodman,M. F., Hanaoka,F., Hinkle,D., Kunkel,T.A., Lawrence,C. W., Livneh,Z., Nohmi,T. *et al.* (2001) The Y-family of DNA polymerases. *Mol. Cell*, **8**, 7–8.
2. Prakash,S. and Prakash,L. (2002) Translesion DNA synthesis in eukaryotes: a one- or two-polymerase affair. *Genes Dev.*, **16**, 1872–1883.
3. Prakash,S., Johnson,R. E. and Prakash,L. (2005) Eukaryotic translesion synthesis DNA polymerases: specificity of structure and function. *Annu. Rev. Biochem.*, **74**, 317–353.
4. Pryor,J. M., Dieckman,L. M., Boehm,E. M. and Washington,M. T. (2014) Eukaryotic Y-family polymerases: a biochemical and structural perspective. *Nucleic Acids Mol. Biol.*, **30**, 85–108.
5. Sale,J. E., Lehmann,A. R. and Woodgate,R. (2012) Y-family DNA polymerases and their role in tolerance of cellular DNA damage. *Nat. Rev. Mol. Cell Biol.*, **13**, 141–152.
6. Wojtaszek,J., Lee,C. J., D'Souza,S., Minesinger,B., Kim,H., D'Andrea,A. D., Walker,G. C. and Zhou,P. (2012) Structural basis of Rev1-mediated assembly of a quaternary vertebrate translesion polymerase complex consisting of Rev1, heterodimeric polymerase (Pol) zeta, and Pol kappa. *J. Biol. Chem.*, **287**, 33836–33846.
7. Wojtaszek,J., Liu,J., D'Souza,S., Wang,S., Xue,Y., Walker,G. C. and Zhou,P. (2012) Multifaceted recognition of vertebrate Rev1 by translesion polymerases zeta and kappa. *J. Biol. Chem.*, **287**, 26400–26408.
8. Haracska,L., Kondratick,C. M., Unk,I., Prakash,S. and Prakash,L. (2001) Interaction with PCNA is essential for yeast DNA polymerase eta function. *Mol. Cell*, **8**, 407–415.
9. Haracska,L., Johnson,R. E., Unk,I., Phillips,B., Hurwitz,J., Prakash,L. and Prakash,S. (2001) Physical and functional interactions of human DNA polymerase eta with PCNA. *Mol. Cell. Biol.*, **21**, 7199–7206.
10. Haracska,L., Johnson,R. E., Unk,I., Phillips,B. B., Hurwitz,J., Prakash,L. and Prakash,S. (2001) Targeting of human DNA polymerase iota to the replication machinery via interaction with PCNA. *Proc. Natl. Acad. Sci. U.S.A.*, **98**, 14256–14261.
11. Haracska,L., Unk,I., Johnson,R. E., Phillips,B. B., Hurwitz,J., Prakash,L. and Prakash,S. (2002) Stimulation of DNA synthesis activity of human DNA polymerase kappa by PCNA. *Mol. Cell. Biol.*, **22**, 784–791.
12. Guo,C., Sonoda,E., Tang,T. S., Parker,J. L., Bielen,A. B., Takeda,S., Ulrich,H. D. and Friedberg,E. C. (2006) REV1 protein interacts with PCNA: significance of the REV1 BRCT domain in vitro and in vivo. *Mol. Cell*, **23**, 265–271.
13. Acharya,N., Yoon,J. H., Gali,H., Unk,I., Haracska,L., Johnson,R. E., Hurwitz,J., Prakash,L. and Prakash,S. (2008) Roles of PCNA-binding and ubiquitin-binding domains in human DNA polymerase eta in translesion DNA synthesis. *Proc. Natl. Acad. Sci. U.S.A.*, **105**, 17724–17729.
14. Murakumo,Y., Ogura,Y., Ishii,H., Numata,S., Ichihara,M., Croce,C. M., Fishel,R. and Takahashi,M. (2001) Interactions in the error-prone postreplication repair proteins hREV1, hREV3, and hREV7. *J. Biolo. Chem.*, **276**, 35644–35651.
15. Guo,C., Fischhaber,P. L., Luk-Paszyc,M. J., Masuda,Y., Zhou,J., Kamiya,K., Kisker,C. and Friedberg,E. C. (2003) Mouse Rev1 protein interacts with multiple DNA polymerases involved in translesion DNA synthesis. *EMBO J.*, **22**, 6621–6630.
16. Ohashi,E., Murakumo,Y., Kanjo,N., Akagi,J., Masutani,C., Hanaoka,F. and Ohmori,H. (2004) Interaction of hREV1 with three human Y-family DNA polymerases. *Genes Cells*, **9**, 523–531.
17. Acharya,N., Haracska,L., Prakash,S. and Prakash,L. (2007) Complex formation of yeast Rev1 with DNA polymerase eta. *Mol. Cell. Biol.*, **27**, 8401–8408.

18. Ohashi,E., Hanafusa,T., Kamei,K., Song,I., Tomida,J., Hashimoto,H., Vaziri,C. and Ohmori,H. (2009) Identification of a novel REV1-interacting motif necessary for DNA polymerase kappa function. *Genes Cells*, **14**, 101–111.
19. Pozhidaeva,A., Pustovalova,Y., D'Souza,S., Bezsonova,I., Walker,G. C. and Korzhnev,D. M. (2012) NMR structure and dynamics of the C-terminal domain from human Rev1 and its complex with Rev1 interacting region of DNA polymerase eta. *Biochemistry*, **51**, 5506–5520.
20. Moldovan,G. L., Pfander,B. and Jentsch,S. (2007) PCNA, the maestro of the replication fork. *Cell*, **129**, 665–679.
21. Dieckman,L. M., Freudenthal,B. D. and Washington,M. T. (2012) PCNA structure and function: insights from structures of PCNA complexes and post-translationally modified PCNA. *Subcell. Biochem.*, **62**, 281–299.
22. Krishna,T. S., Kong,X. P., Gary,S., Burgers,P. M. and Kuriyan,J. (1994) Crystal structure of the eukaryotic DNA polymerase processivity factor PCNA. *Cell*, **79**, 1233–1243.
23. Jonsson,Z. O., Hindges,R. and Hubscher,U. (1998) Regulation of DNA replication and repair proteins through interaction with the front side of proliferating cell nuclear antigen. *EMBO J.*, **17**, 2412–2425.
24. Warbrick,E. (2000) The puzzle of PCNA's many partners. *Bioessays*, **22**, 997–1006.
25. Maga,G. and Hubscher,U. (2003) Proliferating cell nuclear antigen (PCNA): a dancer with many partners. *J. Cell Sci.*, **116**, 3051–3060.
26. Nelson,J. R., Lawrence,C. W. and Hinkle,D. C. (1996) Deoxycytidyl transferase activity of yeast REV1 protein. *Nature*, **382**, 729–731.
27. Washington,M. T., Minko,I. G., Johnson,R. E., Haracska,L., Harris,T. M., Lloyd,R. S., Prakash,S. and Prakash,L. (2004) Efficient and error-free replication past a minor-groove N2-guanine adduct by the sequential action of yeast Rev1 and DNA polymerase zeta. *Mol. Cell. Biol.*, **24**, 6900–6906.
28. Haracska,L., Prakash,S. and Prakash,L. (2002) Yeast Rev1 protein is a G template-specific DNA polymerase. *J. Biol. Chem.*, **277**, 15546–15551.
29. Pryor,J. M. and Washington,M. T. (2011) Pre-steady state kinetic studies show that an abasic site is a cognate lesion for the yeast Rev1 protein. *DNA Repair*, **10**, 1138–1144.
30. Nelson,J. R., Gibbs,P. E., Nowicka,A. M., Hinkle,D. C. and Lawrence,C. W. (2000) Evidence for a second function for Saccharomyces cerevisiae Rev1p. *Mol. Microbiol.*, **37**, 549–554.
31. Ohmori,H., Hanafusa,T., Ohashi,E. and Vaziri,C. (2009) Separate roles of structured and unstructured regions of Y-family DNA polymerases. *Adv. Protein Chem. Struct. Biol.*, **78**, 99–146.
32. Johnson,R. E., Prakash,S. and Prakash,L. (1999) Efficient bypass of a thymine-thymine dimer by yeast DNA polymerase, Poleta. *Science*, **283**, 1001–1004.
33. Haracska,L., Yu,S. L., Johnson,R. E., Prakash,L. and Prakash,S. (2000) Efficient and accurate replication in the presence of 7,8-dihydro-8-oxoguanine by DNA polymerase eta. *Nat. Genet.*, **25**, 458–461.
34. Johnson,R. E., Kondratick,C. M., Prakash,S. and Prakash,L. (1999) hRAD30 mutations in the variant form of xeroderma pigmentosum. *Science*, **285**, 263–265.
35. Masutani,C., Kusumoto,R., Yamada,A., Dohmae,N., Yokoi,M., Yuasa,M., Araki,M., Iwai,S., Takio,K. and Hanaoka,F. (1999) The XPV (xeroderma pigmentosum variant) gene encodes human DNA polymerase eta. *Nature*, **399**, 700–704.
36. Boehm,E. M., Powers,K.T., Kondratcik,C.M., Spies,M., Houtman,J.C.D. and Washington,M.T. (2016) The PCNA-interacting protein (PIP) motif of DNA polymerase eta mediates its interaction with the C-terminal domain of Rev1. *J. Biol. Chem.*, **291**, 8735–8744.
37. Washington,M. T., Prakash,L. and Prakash,S. (2001) Yeast DNA polymerase eta utilizes an induced-fit mechanism of nucleotide incorporation. *Cell*, **107**, 917–927.
38. Haracska,L., Unk,I., Johnson,R. E., Johansson,E., Burgers,P. M., Prakash,S. and Prakash,L. (2001) Roles of yeast DNA polymerases delta and zeta and of Rev1 in the bypass of abasic sites. *Genes Dev.*, **15**, 945–954.
39. Freudenthal,B. D., Ramaswamy,S., Hingorani,M. M. and Washington,M. T. (2008) Structure of a mutant form of proliferating cell nuclear antigen that blocks translesion DNA synthesis. *Biochemistry*, **47**, 13354–13361.
40. Ghoneim,M. and Spies,M. (2014) Direct correlation of DNA binding and single protein domain motion via dual illumination fluorescence microscopy. *Nano Lett.*, **14**, 5920–5931.
41. Honda,M., Park,J., Pugh,R. A., Ha,T. and Spies,M. (2009) Single-molecule analysis reveals differential effect of ssDNA-binding proteins on DNA translocation by XPD helicase. *Mol. Cell*, **35**, 694–703.
42. Masuda-Ozawa,T., Hoang,T., Seo,Y. S., Chen,L. F. and Spies,M. (2013) Single-molecule sorting reveals how ubiquitylation affects substrate recognition and activities of FBH1 helicase. *Nucleic Acids Res.*, **41**, 3576–3587.
43. Haghighat Jahromi,A., Honda,M., Zimmerman,S. C. and Spies,M. (2013) Single-molecule study of the CUG repeat-MBNL1 interaction and its inhibition by small molecules. *Nucleic Acids Res.*, **41**, 6687–6697.
44. Cordes,T., Vogelsang,J. and Tinnefeld,P. (2009) On the mechanism of Trolox as antiblinking and antibleaching reagent. *J. Am. Chem. Soc.*, **131**, 5018–5019.
45. Zhou,R., Kunzelmann,S., Webb,M. R. and Ha,T. (2011) Detecting intramolecular conformational dynamics of single molecules in short distance range with subnanometer sensitivity. *Nano Lett.*, **11**, 5482–5488.
46. Milescu,L. S., Nicolai,C. L., Qin,F. and Sachs,F. (2002) New developments in the QUB software for single-channel data analysis. *Biophys. J.*, **82**, 267A.
47. Pustovalova,Y., Maciejewski,M. W. and Korzhnev,D. M. (2013) NMR mapping of PCNA interaction with translesion synthesis DNA polymerase Rev1 mediated by Rev1-BRCT domain. *J. Mol. Biol.*, **425**, 3091–3105.
48. Kulak,N. A., Pichler,G., Paron,I., Nagaraj,N. and Mann,M. (2014) Minimal, encapsulated proteomic-sample processing applied to copy-number estimation in eukaryotic cells. *Nat. Methods*, **11**, 319–324.
49. Ghaemmaghami,S., Huh,W. K., Bower,K., Howson,R. W., Belle,A., Dephoure,N., O'Shea,E. K. and Weissman,J. S. (2003) Global analysis of protein expression in yeast. *Nature*, **425**, 737–741.
50. Watanabe,K., Tateishi,S., Kawasuji,M., Tsurimoto,T., Inoue,H. and Yamaizumi,M. (2004) Rad18 guides poleta to replication stalling sites through physical interaction and PCNA monoubiquitination. *EMBO J.*, **23**, 3886–3896.
51. Hoege,C., Pfander,B., Moldovan,G. L., Pyrowolakis,G. and Jentsch,S. (2002) RAD6-dependent DNA repair is linked to modification of PCNA by ubiquitin and SUMO. *Nature*, **419**, 135–141.
52. Stelter,P. and Ulrich,H. D. (2003) Control of spontaneous and damage-induced mutagenesis by SUMO and ubiquitin conjugation. *Nature*, **425**, 188–191.
53. Kuang,L., Kou,H., Xie,Z., Zhou,Y., Feng,X., Wang,L. and Wang,Z. (2013) A non-catalytic function of Rev1 in translesion DNA synthesis and mutagenesis is mediated by its stable interaction with Rad5. *DNA Repair*, **12**, 27–37.
54. Essers,J., Theil,A. F., Baldeyron,C., van Cappellen,W. A., Houtsmuller,A. B., Kanaar,R. and Vermeulen,W. (2005) Nuclear dynamics of PCNA in DNA replication and repair. *Mol. Cell. Biol.*, **25**, 9350–9359.